Astron. Astrophys. 285, 648–654 (1994)

ASTRONOMY AND ASTROPHYSICS

The deep layers of solar magnetic elements

U. Grossmann-Doerth[1], M. Knölker[1], M. Schüssler[1], and S.K. Solanki[2]

[1] Kiepenheuer-Institut für Sonnenphysik, Schöneckstr. 6, D-79104 Freiburg, Germany
[2] Institut für Astronomie, ETH–Zentrum, CH-8092 Zürich, Switzerland

Received 5 August 1993 / Accepted 13 November 1993

Abstract. We compare self-consistent theoretical models of solar magnetic flux sheets with spectropolarimetric observations of a solar plage and a network region. Our observational diagnostics mainly provide information on temperature and magnetic field of the deep photospheric layers. They are used to constrain the two free parameters of the models, viz. width and initial evacuation of the flux sheets. We find that the width of flux sheets in the network is approximately 200 km, while it is 300–350 km in an active plage. The flux sheets turn out to be less evacuated than previously thought, so they have continuum intensities close to unity. Since these are average values, however, our results do not exclude the presence of either smaller and brighter or larger and darker magnetic structures.

Key words: Sun: magnetic fields – Sun: faculae – Sun: activity – MHD

1. Introduction

The magnetic and thermodynamic structure of small-scale solar magnetic features has been the subject of extensive investigations. Two different approaches have been used for developing models of these structures. On the one hand theoretical models have been derived which aim at a fully self-consistent solution of the MHD equations, but must often make a number of simplifying assumptions to achieve computational tractability (e.g. Spruit 1976; Deinzer et al. 1984a,b; Knölker et al. 1988; Knölker & Schüssler 1988; Steiner 1990; Knölker et al. 1991; Pizzo et al. 1993; see reviews by Schüssler 1990 and Spruit et al. 1992). The empirical models, on the other hand, are based on observational data which are used to constrain numerous free parameters (e.g. Solanki 1986; Walton 1987; Keller et al. 1990; see reviews by Stenflo 1989; Solanki 1990, 1993). In the past, theoretical models have been compared to observations only indirectly, i.e., the temperature and magnetic field profiles of the theoretical models have been compared with the relevant quantities obtained from empirical models. Since the latter are subject to a number of restrictive assumptions (e.g., temperature and magnetic field strength are assumed to be constant at a given geometrical height within the magnetic feature) this procedure is hardly satisfactory.

It is the purpose of the present work to put the modelling of solar flux tubes on a firmer basis by directly comparing observed Stokes V profiles with those which are computed from theoretical models. We use two-dimensional dynamic flux sheet models which take magnetic tension and partial ionisation effects fully into account and which include a proper grey radiative transfer. We consider a set of models with diverse values of their free parameters, namely initial size and gas pressure, and compare their temperature and magnetic field strength signatures with observation in order to constrain the value of the free parameters. We restrict the analysis to the deep atmospheric layers since the models are most reliable there. At greater heights, effects due to the non-greyness of the absorption coefficient and, probably, mechanical heating by waves, both of which are not included in the present models, become important.

In Sect. 2 we give a brief overview of the MHD models and describe observations and diagnostic procedure in Sect. 3. The results are presented and discussed in Sect. 4. We summarize our conclusions in Sect. 5.

2. Models

The models are the result of numerical integration of the time-dependent MHD equations in two-dimensional Cartesian geometry; they represent magnetic *flux sheets*, i.e. infinitely extended slabs of magnetic flux thought to represent the organisation of magnetic fields within elongated intergranular lanes. The original version of the code has been described by Deinzer et al. (1984a). Since then a number of improvements has been incorporated, most notably the treatment of energy transport by radiation by a full (grey, LTE) radiative transfer calculation using Feautrier integration along a large number of rays of various inclination and azimuth angles. A detailed description of the methods and the results of various test calculations will be given in a forthcoming paper. First results have been presented by Grossmann-Doerth et al. (1989) and Knölker et al. (1991). The simulation solves

Send offprint requests to: M. Schüssler

- Momentum equations (vertical, horizontal), including inertial force, pressure force, gravity, magnetic (Lorentz) force and viscous force,
- Equation of continuity (fully compressible),
- Induction equation,
- Energy equation, including advection and compression, radiation, turbulent entropy diffusion, and effects of partial ionization.

The material functions (like specific heat, molecular weight, opacity) are determined self-consistently as functions of temperature and pressure in the course of the time-dependent simulation. The numerical scheme used is based on an implicit version of the *Moving Finite Element* method (Gelinas et al. 1981). In order to resolve steep gradients near the edge of the simulated flux concentration, the node points are distributed non-uniformly and follow the motion of the thin transition layer between the magnetic element and its environment during the dynamical evolution.

'Open' or 'closed' boundary conditions for velocity and temperature can be used at the top and bottom boundaries. The magnetic field is vertical at all boundaries. Turbulent entropy diffusion by unresolved small-scale motions is accounted for by a mixing length formalism. This kind of energy transport is completely suppressed in the magnetic structures by a suitable dependence on magnetic field strength (for more details see Deinzer et al. 1984a). The coefficients of (turbulent) viscosity and magnetic diffusivity have been chosen to be as small as possible while still preserving numerical stability. This leads to hydrodynamic Reynolds numbers between 10^3 and 10^4. The magnetic diffusivity is set to zero which facilitates greatly the control of node point motion. Test calculations have shown that the resulting models are essentially unchanged if we calculate with magnetic Reynolds numbers of the order of the hydrodynamic Reynolds numbers given above. The width of the transition layer between magnetic structure and environment is taken as one tenth of the (initial) half width of the flux sheet. As long as this ratio is small compared to unity, the resulting magnetic and thermal structures do not significantly depend on the choice of this parameter (Knölker et al. 1988).

The remaining free parameters of the models are initial density in the flux sheet and its total magnetic flux (per unit length) which determines its horizontal width. The flux sheet models which are used in this paper are specified in Table 1. All models have been evolved in time until a stationary state was reached which shows a strong external downflow near the flux sheet and oscillations with a period of about 4 minutes within the flux sheet. Here we shall concern ourselves with the properties of the resulting models in deep layers which do not change significantly with oscillation phase. For the purpose of illustration we show in Fig. 1 a cross section of model M350.

The quantities of interest in this paper are magnetic field strength B_0 and temperature T_0 at continuum optical depth $\tau_c = 1$ (for 5000 Å). Both quantities depend differently on our model parameters w (horizontal width of the flux sheet at $\tau_c = 1$ of the external atmosphere) and α (evacuation parameter, see caption of Table 1 for a definition). For a given value of α the temperature T_0 *decreases* with growing width since the flux sheet becomes more opaque and is therefore less efficiently heated by radiation from the side. At the same time, the field strength B_0 *increases* since the surface $\tau_c = 1$ in the flux sheet moves downward due to the temperature sensitivity of the continuum opacity. On the other hand, for a given width both temperature and field strength decrease for increasing values of α (larger internal density) since the surface $\tau_c = 1$ moves upward. These different dependences allow a combination of values (w, α) to be determined in a unique way for a given (observed) pair T_0, B_0 (or a pair of observations which are sensitive to these quantities).

Table 1. Parameters and properties of the set of flux sheet models used in this paper. Parameters are w and α: w is the (full) width of the sheet at a height which corresponds to continuum optical depth unity of the external medium far away from the flux sheet; the evacuation parameter $\alpha = \rho_{i0}/\rho_{e0}$ is the initial ratio of internal to external density (temperature equal to undisturbed atmospheric model, flux sheet in horizontal pressure equilibrium). Some properties of the resulting stationary models are also given: temperature (T_0) and magnetic field strength (B_0) at continuum optical depth $\tau_c = 1$ at the center of the flux sheet and continuum intensity I_c at 5000 Å averaged over the magnetic structure in units of the continuum intensity I_0 of the undisturbed atmosphere.

Model	w (km)	α	T_0 (K)	B_0 (G)	$\langle I_c \rangle / I_0$
M130	100	0.3	7100	2300	1.70
M150	100	0.5	6580	1800	1.12
M230	200	0.3	6880	2550	1.50
M250	200	0.5	6230	1940	1.01
M350	300	0.5	6060	1980	0.94
M430	400	0.3	6480	2730	1.19
M450	400	0.5	5930	2270	0.86
M460	400	0.6	5680	1940	0.70
M850	800	0.5	5720	2200	0.78

3. Observational data and diagnostic tools

The observational data used are measurements of Stokes V profiles of two visible Fe I lines (5250.20 Å and 5247.06 Å), two C I lines (5380.32 Å and 5052.15 Å), three Fe II lines (5132.66 Å, 5325.56 Å and 5414.07 Å) and the infrared Fe I line at 15648.52 Å, recorded near disc center in both a network region (small Stokes V signal, i.e. small magnetic filling factor) and a plage (larger Stokes V signal), with the McMath telescope at Kitt Peak. The visible data and some of the infrared data were obtained with the Fourier Transform Spectrometer; for more details refer to Stenflo et al. (1984) and Solanki (1987). The observations of the 15648 Å line were partly obtained with the vertical spectrograph of the McMath telescope (see Solanki et al. 1992 and Rüedi et al. 1992 for details) and are not cospatial to the visible data. However, the splitting of these lines appears to depend only on the Stokes V amplitude (i.e. filling factor), and even that only relatively weakly (Rüedi et al. 1992; Rabin 1992). Consequently, we have used the splittings expected for

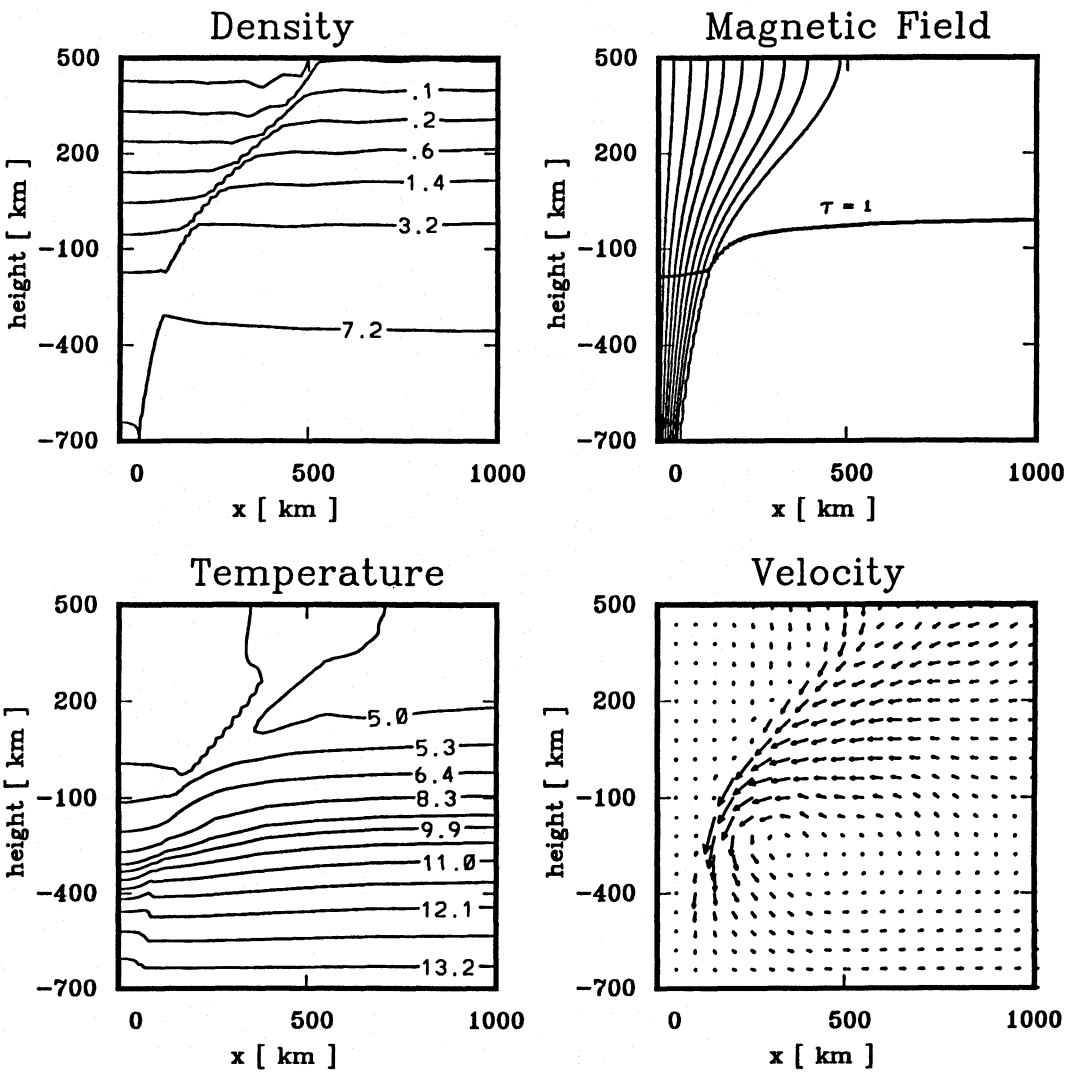

Fig. 1. Properties of the flux sheet model M350. Only half of the symmetric structure is shown; the sheet's properties do not vary in the direction perpendicular to the plane of the figure. Densities are in units of 10^{-7} g cm^{-3}, temperatures in 1000 K. The level at which the continuum optical depth at 5000 Å is unity is indicated in the magnetic field plot. The velocity arrows scale with the modulus of the velocity; the maximum velocity in the downflow jet adjacent to the flux sheet is about 4 km s^{-1}. The temperature structure in the upper levels of the flux sheet (above $\sim$ 100 km) varies strongly in the course of the internal oscillation; however, the layers around $\tau_c = 1$ are barely affected

the filling factors corresponding to the regions observed in the visible. The Stokes V formation heights of the eight lines for a vertical line of sight through the center of model M350 are shown in Fig. 2.

As diagnostic tool for the temperature in the deep layers of our models we use the C I/Fe II Stokes V 'line ratios' proposed by Solanki & Brigljević (1992). The Stokes V line ratio R_l of two spectral lines 1 and 2 is defined by $R_l = (V_{1r} + V_{1b})/(V_{2r} + V_{2b})$ where V_i denotes the absolute value of the red (index r) or the blue (index b) extremum of Stokes V of line i (Stenflo 1973; Solanki 1993). As can be seen from Fig. 2 the C I lines are formed in a relatively narrow depth range deep in the atmosphere. Because of their high ionization and excitation energies the C I lines are very sensitive to temperature changes, while the Fe II lines are not. Thus the C I/Fe II line ratio is a good temperature indicator for deep atmospheric layers as illustrated in Fig. 3 where the six line ratios which can be defined with our C I and Fe II lines are plotted versus a (height-independent) temperature increment in the quiet solar atmosphere. We use line ratios because they are independent of the unknown magnetic 'filling factor', i.e. the number density of magnetic structures in the observed area. Once a correct model flux tube has been derived from a given set of observations, the filling factor can, in principle, be derived by comparing the observed Stokes V amplitudes (or areas) with those arising from the model.

It should be noted, however, that these line ratios are not independent of magnetic field strength as may be seen in Fig. 4. This may lead to ambiguity as is illustrated in Fig. 5 which shows points of equal value of line ratios as function of temperature (at $\tau_c = 1$) and magnetic field strength. In principle, the effect of a temperature increment on the line ratios could be cancelled by

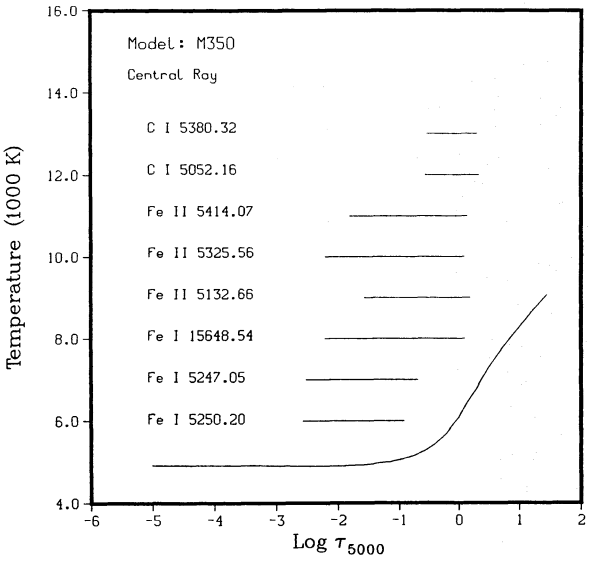

Fig. 2. Temperature and Stokes V height of formation of the spectral lines used in our analysis in the center of Model M350. The height of formation is defined as the range where the line depression contribution functions (Magain 1986; Grossmann-Doerth et al. 1988) of the specified wavelength interval are larger than 50% of their maximum value. In the present case this wavelength interval covers the range where Stokes V is larger than 50% of its maximum value

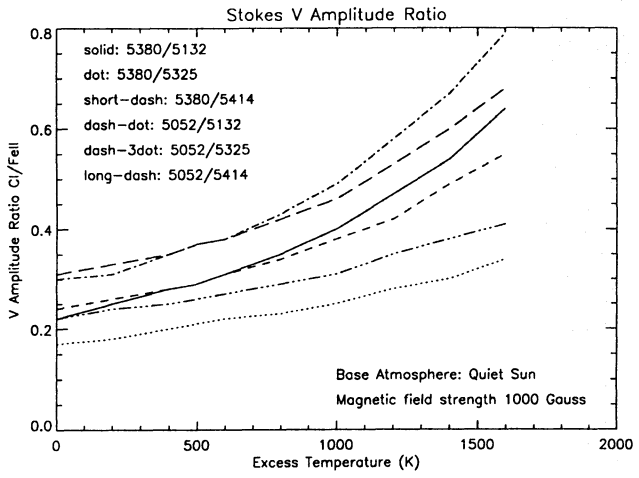

Fig. 3. Stokes V C I/Fe II line ratios as function of a height-independent temperature excess with respect to a model of the quiet sun. A uniform magnetic field of 1000 G is assumed to be present

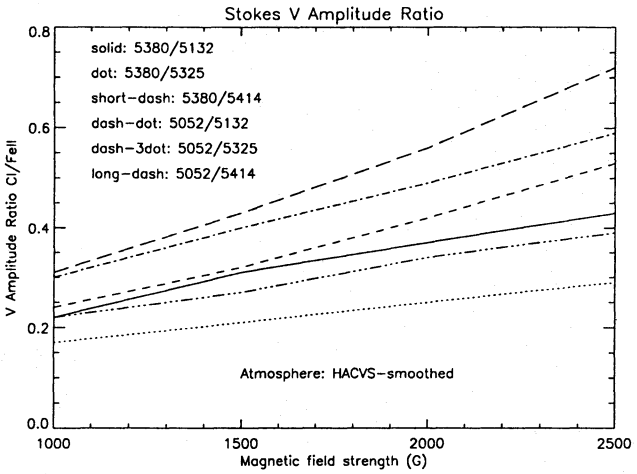

Fig. 4. Stokes V C I/Fe II line ratios as function of strength of a uniform magnetic field. A model of the quiet sun has been used for the other atmospheric quantities

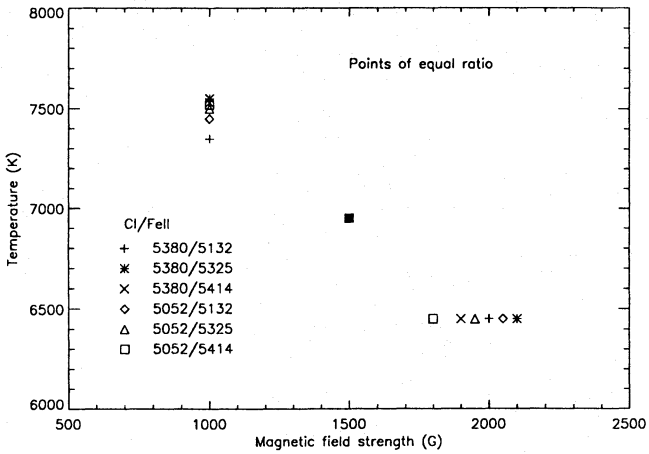

Fig. 5. Loci of equal values of line ratio. Starting with the line ratio for 1500 G and 6900 K at $\tau_c = 1$ the plot shows the temperature values (at $\tau_c = 1$) for 1000 G and the magnetic field strength values for 6300 K (at $\tau_c = 1$) for which the line ratios assume the same values. Note that, for example, the effect of a temperature increase on the value of the line ratios may be cancelled by a suitable reduction of the magnetic field strength

a decrease in magnetic field and vice versa. We eliminate this ambiguity by including in our set of observables two quantities which depend exclusively on magnetic field strength: First, the 'magnetic line ratio' Fe I 5250/Fe I 5247 and, second, the Zeeman splitting of the infrared line Fe I 15648.518 Å. The dependence of the Fe I 5250/Fe I 5247 line ratio on temperature is negligible because the lines have almost identical excitation potential and line strength. The infrared line Fe I 15648 is a good diagnostic tool for the magnetic field strength since it is completely split even in moderately strong magnetic fields because of both its large wavelength and its large Landé factor. In order to demonstrate its diagnostic value we have determined, for various flux sheet models, the optical depth at which the magnetic field assumes the value which corresponds to the wavelength seperation of the peaks of Stokes V (averaged over the flux sheet) of the line. The result is shown in Table 2. It is remarkable how little this optical depth varies although the models are quite different. Thus we conclude that the magnetic field strength at $\tau_c \approx 0.1$ can be obtained in a fairly reliable way from the wavelength seperation of the peaks of the Stokes V profile averaged over the flux sheet.

Table 2. Characteristic optical depth x_B of the spectral line Fe I 15648 in various flux sheet models. $x = \log \tau_{5000}$ is the logarithm of the continuum optical depth at 5000 Å and x_B is defined as the value of x where the magnetic field in the center of the flux sheet assumes the value which is obtained from the wavelength separation of the peaks of the composite Stokes V profiles (averages over the flux sheet). $\Delta\lambda$ is the wavelength difference between the Stokes V peaks and B the corresponding field strength.

Model	$\Delta\lambda$ (Å)	B (G)	x_B
M130	1.30	1900	-0.85
M150	0.92	1360	-1.0
M230	1.50	2300	-0.85
M250	1.10	1620	-0.80
M350	0.95	1400	-1.0
M430	1.55	2280	-0.85
M450	1.33	1960	-0.85
M460	1.12	1650	-0.85
M850	1.25	1860	-0.85

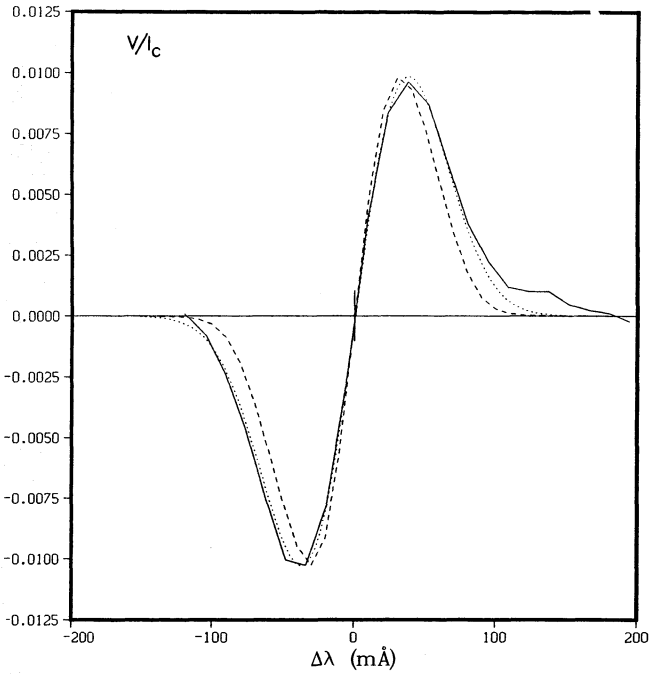

Fig. 6. Stokes V profiles of FeII 5414.07 Å. Solid: Observed in a plage region. Dashed: Computed average of Model M350, normalized in order that the blue peak equals the observed value. Dotted: Computed profile broadened by a macroturbulent velocity (Aller 1963) of 1.5 km/s; this profile has also been normalized

4. Results

For all the eight spectral lines and the models given in Table 1 we have computed the profiles of Stokes V for a large number (normally 25) of rays at normal incidence, evenly spaced across the flux sheet. For comparison with the observations we used the average of these profiles divided by the average of the emerging continuum intensity. Similar to earlier results to reproduce observed Stokes V profiles with the aid of flux tube models it was found that for all except the visible Fe I lines the computed profiles were narrower than the observed ones. Therefore we broadened the synthetic Stokes V profiles by a macroturbulent velocity (Aller 1963) whose value was chosen to achieve maximum agreement between observed and computed profiles; the resulting velocities lie in the range of 1 to 2 km/s. For the purpose of illustration we show in Fig. 6 observed and computed Stokes V profiles of the line FeII 5132.67 Å.

Observed and calculated line ratios and Stokes V peak separation of the infrared line are shown in Table 3. As expected from Fig. 3, the C I/Fe II line ratios are larger for the hotter, i.e. less dense, models. As a measure for the agreement between observation and model we use χ^2, the sum of the squared differences between calculated and measured values for the six C I/Fe II line ratios, normalized to the minimum value. This quantity has been determined separately for the plage and the network data. The models with the smallest χ^2 are considered to represent the data best. From inspection of the values of the normalized χ^2 in Table 3 we find that model M250 (a flux sheet with 200 km width and $\alpha = 0.5$) provides the best fit to the network data while models M350 and M450 (300 km and 400 km width, respectively, and also $\alpha = 0.5$) represent the plage data equally well. Note that the minima of χ^2 and thus the models with optimum fit are well defined.

We can use the Stokes V peak separation of the fully split infrared line (last column in Table 3) in order to decide between the two models which both provide a good fit to the C I/Fe II line ratios from the plage data. While model M350 ($B_0 = 1980$ G) shows a smaller separation than the data (0.95 Å vs. 1.10 Å) the value of 1.33 Å for M450 is definitely too large and indicates that the magnetic field ($B_0 = 2270$ G at $\tau_c = 1.$) is too strong. A less evacuated flux sheet model (M460) would yield a better agreement with the observed splitting of the infrared line; however this model would be definitely too cool. We therefore conclude that model M350 is the best representative of the 'typical' magnetic structure in a plage. We expect a model lying between M350 and M450 to do even better (the Zeeman splitting is too small for M350 and too large for M450). We have been refraining, however, from such fine-tuning of the model parameters. Since the peak separation of M250, on the other hand, is consistent with the value observed in the network we consider that model as an adequate representation of the 'typical' network structure.

The 5250/5247 magnetic line ratio gives independent evidence that the strongly evacuated models ($\alpha = 0.3$) are not realistic since the line ratios of these models are significantly smaller than the observed values (0.74 for both network and plage). This is due to the strong magnetic fields of these models, possibly in combination with their larger temperature: although the line ratio is not directly dependent on temperature, the line pair is formed deeper (i.e., in a layer of larger field strength) in a hot atmosphere due to the line weakening effect (Steiner & Pizzo 1989). The values for M130 (0.58) and M230 (0.61) are even smaller than 2/3, the ratio of the Landé factors of the lines. The reason for this lies in the larger magnetic field gra-

Table 3. Observed and calculated Stokes V line ratios and Stokes V peak separation $\Delta\lambda$ of the Fe I infrared line. The models are specified in Table 1. χ^2 denotes the sum of the squared differences between observed and calculated C I/Fe II Stokes V line ratios, normalized to their respective minimum value.

	5380/ 5132	5380/ 5325	5380/ 5414	5052/ 5132	5052/ 5325	5052/ 5414	χ^2 (Network)	χ^2 (Plage)	5250/ 5247	$\Delta\lambda$ (Å)
Network	.40	.26	.40	.50	.33	.48			.74	0.98
Plage	.31	.20	.31	.44	.29	.44			.74	1.10
M130	.64	.39	.64	.81	.50	.80	105.7	99.0	.58	1.30
M150	.41	.31	.45	.53	.40	.56	5.1	13.4	.68	0.92
M230	.47	.30	.49	.63	.41	.66	20.7	29.3	.61	1.50
M250	.38	.23	.38	.52	.30	.50	1.0	3.7	.67	1.00
M350	.29	.21	.31	.38	.28	.40	13.5	1.0	.72	0.95
M430	.45	.29	.50	.58	.37	.63	12.9	22.1	.66	1.55
M450	.27	.19	.31	.38	.27	.44	14.6	1.0	.68	1.33
M460	.22	.17	.26	.29	.22	.34	40.0	8.6	.70	1.12
M850	.23	.16	.26	.32	.22	.35	35.3	6.7	.70	1.20

dient of the more strongly evacuated flux sheets which leads to a stronger broadening of the Stokes V wings of Fe I 5250 compared to Fe I 5247.

5. Discussion and conclusions

From the results presented in the preceding section we conclude that, as far as the layers around optical depth unity are concerned, model M250 (a flux sheet with 200 km width and an initial evacuation parameter of $\alpha = 0.5$) is consistent with the diagnostics formed on the basis of the network data while model M350 (300 km width, $\alpha = 0.5$) represents the observational data for plage data best. Flux sheets with significantly different widths and models with different evacuation all fail to satisfy the constraints set by our temperature and magnetic field diagnostics.

The average continuum intensity emerging from the flux sheet divided by that of the average quiet Sun of these models is unity for M250 and 0.94 for M350. We thus confirm the result of Solanki & Brigljević (1992) that the continuum intensity of magnetic structures in plages is smaller than that of the average photosphere. For the network structures, however, these authors find indications for a somewhat larger value of the continuum intensity.

We do not think that there is a contradiction between our results and the existence of magnetic 'bright points' with continuum contrasts significantly larger than unity (e.g. Keller 1992). There are indeed indications that magnetic structures in network and plages show a distribution of sizes and continuum contrasts (Spruit & Zwaan 1981; Zirin & Wang 1992; Keller 1992). Our results indicate that the major part of the magnetic flux in both cases resides in structures with no conspicuous intensity contrast but they do not exclude that some fraction of the magnetic flux is in small, very bright structures which may be described by our models with smaller widths and large continuum contrasts (M130 or M150). The same applies to larger and darker structures. The 'typical' structures, however, should be similar to our models M250 (network) and M350 (plage).

The main difference between network and plage magnetic structures seems to be a somewhat lower temperature of the latter. In our models this results from the larger width which decreases the efficiency of lateral radiative heating. We must keep in mind, however, that our models are *isolated* structures. If the filling factor becomes large we may expect that the overall convective energy transport is disturbed by the densely packed magnetic structures so that the surroundings of the flux elements are cooler than for an isolated network element. This would also reduce the efficiency of radiative heating and lead to cooler structures. Since simulations for sheet or tube arrays are presently not available we cannot definitely state that the lower temperature of plage magnetic structures is due to a larger diameter. We have shown, however, that this possibility cannot be excluded since we have been able to construct models which are fully compatible with the observational data.

A last remark may concern the question of flux sheets vs. flux tubes. Although elongated structures are often observed in intergranular lanes (e.g. von der Lühe 1987) the model of a flux sheet is certainly an idealization. We may assume from geometrical considerations that for a cylindrical flux tube radiative heating is probably somewhat more efficient than for a flux sheet of the same diameter (width). Therefore, flux *tube* models which are consistent with the observational diagnostics discussed above would probably be somewhat *larger* than our flux sheets, though not drastically so as a comparison between our models and the tube models of Steiner (1990) suggests.

References

Aller, L.H.: Astrophysics - The Atmosphere of the Sun and Stars, The Ronald Press Company New York, Second Edition 1963, p.388
Deinzer W., Hensler G., Schüssler M., Weisshaar E., 1984a, A&A 139, 426

Deinzer W., Hensler G., Schüssler M., Weisshaar E., 1984b, A&A 139, 435

Gelinas R.J., Doss S.K., Miller K., 1981, J. Comp. Phys. 40, 202

Grossmann-Doerth U., Larsson B., Solanki S.K., 1988, A&A 204, 266

Grossmann-Doerth U., Knölker M., Schüssler M., Weisshaar E., 1989 in Solar and Stellar Granulation, R.J. Rutten and G. Severino (Eds.), Kluwer Drdrecht, p. 191

Keller C.U., 1992, Nature, 359, 307

Keller C.U., Solanki S.K., Steiner O., Stenflo J.O., 1990, A&A 233, 583

Knölker M., Schüssler M., 1988, A&A 202, 275

Knölker M., Schüssler M., Weisshaar E., 1988, A&A 194, 257

Knölker M., Grossmann-Doerth U., Schüssler M., Weisshaar E., 1991, Adv. Space Res. 11, 285

Magain P., 1986, A&A 163, 135

Pizzo V.J., McGregor K.B., Kunasz P.B., 1993, ApJ 404, 788

Rabin D., 1992b, ApJ 391, 832

Rüedi I., Solanki S.K., Livingston W., Stenflo, J.O., 1992, A&A 263, 323

Schüssler M., 1990, in Solar Photosphere: Structure, Convection and Magnetic Fields, J.O. Stenflo (Ed.), Kluwer, Dordrecht, IAU Symp. 138, p. 161

Solanki S.K., 1986, A&A 168, 311

Solanki S.K., 1987, *Ph.D. Thesis,* No. 8309, ETH, Zürich

Solanki S.K., 1990, in Solar Photosphere: Structure, Convection and Magnetic Fields, J.O Stenflo (Ed.), Kluwer, Dordrecht, IAU Symp. 138, p. 103

Solanki S.K., 1993, Space Sci. Rev., 63, 1

Solanki S.K., Brigljević V., 1992, A&A 262, L29

Solanki S.K., Rüedi I., Livingston W., 1992, A&A 263, 312

Spruit H.C., 1976, Sol. Phys. 50, 269

Spruit H.C., Zwaan C., 1981, Sol. Phys. 70, 207

Spruit H.C., Schüssler M., Solanki S.K., 1992, in Solar Interior and Atmosphere, A.N. Cox, W. Livingston, M.S. Matthews (Eds.), University of Arizona press, Tucson, AZ, p. 890

Steiner O., Pizzo, V.J., 1989, A&A 211, 447

Steiner O., 1990, *Ph.D. Thesis*, No. 9292, ETH-Zürich

Stenflo, J.O., 1973, , Sol. Phys. 32, 41

Stenflo J.O., 1989, A&AR 1, 3

Stenflo J.O., Harvey, J.W., Brault, J.W., Solanki S.K., 1984, A&A 131, 333

Von der Lühe O., 1987, in The Role of Fine-Scale Magnetic Fields on the Structure of the Solar Atmosphere, E.-H. Schröter, M. Vázquez, A.A. Wyller (Eds.), Cambridge University Press, p. 156

Walton S.R., 1987, ApJ 312, 909

Zirin H., Wang H., 1992, ApJ 385, L27

This article was processed by the author using Springer-Verlag TEX A&A macro package 1992.